Pseudogenization of the *cntQ* permease confers distinct yersinopine-metal uptake selectivity in *Yersinia* species

Clémentine Laffont[a,¶], Elizabeth Pradel[b], Laurent Ouerdane[c], Amélie Dewitte[b], Nicolas Oswaldo Gomez[d,§], Mathilde Tribout[a,d], Catherine Brutesco[a], Romé Voulhoux[d], Ryszard Lobinski[c,e], Florent Sebbane[b,*], Pascal Arnoux[a,*]

[a]*Aix Marseille Univ, CEA, CNRS, BIAM, Saint Paul-Lez-Durance, France;* [b]*Univ. Lille, CNRS, Inserm, CHU Lille, Institut Pasteur de Lille, U1019 - UMR 9017 - CIIL - Center for Infection and Immunity of Lille, F-59000 Lille, France;* [c]*Université de Pau et des Pays de l'Adour, e2s UPPA, CNRS, IPREM-UMR5254, Hélioparc, Pau, France ;* [d]*Laboratoire de Chimie Bactérienne (LCB) UMR7283, Institut Microbiologie, Bioénergies et Biotechnologie (IM2B), CNRS, Aix-Marseille Université, Marseille, France.* [e]*Chair of Analytical Chemistry, Warsaw University of Technology, Poland*

¶*Present address: Department of Quantitative Biomedicine, University of Zurich, Winterthurerstrasse 190, 8057 Zürich, Switzerland.*

§*Present address: Department of Molecular Bacteriology, Helmholtz Centre for Infection Research, 38124 Braunschweig, Germany.*

* Florent Sebbane (florent.sebbane@inserm.fr) or Pascal Arnoux (pascal.arnoux@cea.fr

Clémentine Laffont: 0000-0003-3067-1369 ; Elizabeth Pradel: 0000-0003-3563-9325 ; Laurent Ouerdane: 0000-0002-2752-3579 ; Nicolas Oswaldo Gomez: 0000-0001-5723-886X ; Romé Voulhoux: 0000-0002-5258-5958 ; Ryszard Lobinski: 0000-0003-1908-2029 ; Florent Sebbane: 0000-0003-3811-9691 ; Pascal Arnoux: 0000-0003-4609-4893

Statements and Declarations: The authors declare no competing interests.

Acknowledgements

We thank the Agence Nationale de la Recherche for initial support [grants ANR-14-CE09-0007-02 and ANR-20-CE11-0018], the French ministry of research for a PhD grant awarded to CL. FS was partly supported by the ERC Synergy project Synergy-Plague (101118880). We would like to thank Pierre Lê-Bury and Javier Pizarro-Cerda (Institut Pasteur) as well as members of both the Arnoux and Sebbane teams for their support and discussions. Richard C. Allen and Ikram Hammar are acknowledged respectively for his advice on statistical analysis and her initial illustration of the model. S. Preveral and the Ionotec plateform are recognized for their determination of metal content in TMH medium. This article has been deposited to biorxiv (https://doi.org/10.1101/2025.03.14.643292)

Abstract

Yersinopine, a nicotianamine-like metallophore, was recently identified through biochemical analyses, but its *in vivo* production and functional role remain uncharacterized. In *Yersinia pseudotuberculosis* and its recent descendant *Yersinia pestis*, the *cnt* operon (*cntPQRLMI*) putatively encodes the biosynthesis and transport of yersinopine. In *Y. pestis*, however, two frameshift mutations disrupt *cntQ*, which encodes the predicted permease for yersinopine-metal complexes. This pseudogenization raises critical questions about the functional relevance of yersinopine in these closely related species. Here, we show that *cnt* operon expression is repressed by the zinc uptake regulator Zur and that both *Y. pestis* and *Y. pseudotuberculosis* secrete yersinopine under zinc-limited conditions. Unexpectedly, the operon mediates iron uptake in *Y. pseudotuberculosis* but supports zinc acquisition in *Y. pestis*. Moreover, targeted disruption of *cntQ* in *Y. pseudotuberculosis* shifts metal specificity from iron to zinc, mimicking the *Y. pestis* phenotype. Collectively, our results suggest that a single pseudogenization event could rewire metal uptake specificity. Our findings illustrate how evolutionary genome reduction can reshape bacterial physiology.

Keywords: Metal-uptake; ABC transporter; specificity; evolution; Yersinia

50 **Introduction**

51 Metal uptake is fundamental for all living organisms, as metals serve as catalytic and/or structural cofactors
52 for proteins involved in essential metabolic reactions. To efficiently acquire metals, bacteria encode diverse
53 uptake machineries tailored to metal availability in their environmental niches (Ma et al. 2009;
54 Chandrangsu et al. 2017). When metals are abundant or bioavailable, bacteria directly import the free
55 metallic ions through specialized metal-uptake systems, such as ABC transporters (*e.g.,* the ZnuABC
56 transporter responsible for zinc uptake). Under conditions of metal scarcity, metalloregulators of the FUR
57 superfamily (such as Fur for iron or Zur for zinc) modulate gene expression to promote high-affinity
58 acquisition pathways. These include the capture of metal-containing molecules such as haem, or the
59 production, secretion and uptake of specialised molecules called metallophores (such as siderophores),
60 which have a high affinity for metals, opening up new sources that would otherwise be unavailable. These
61 high-affinity pathways are particularly important for pathogenic bacteria facing nutritional immunity, a
62 host defense mechanism that restricts pathogen growth by sequestering essential metals or exposing
63 microbes to toxic metal concentrations (Weinberg 1975; Hood and Skaar 2012; Zygiel and Nolan 2018;
64 Nelson et al. 2021). Among the high-affinity metal acquisition pathways are those involving nicotianamine-
65 like metallophores, such as staphylopine in *Staphylococcus aureus* and pseudopaline in *Pseudomonas*
66 *aeruginosa* (Ghssein et al. 2016; Lhospice et al. 2017). Although initially identified for their broad metal-
67 binding capacities, growing evidence suggests that these metallophores primarily participate in zinc
68 acquisition in metal-chelating host environments (Grim et al. 2017; Mastropasqua et al. 2017; Lhospice et
69 al. 2017). Nevertheless, experimental data also indicate roles in iron or nickel import (Ghssein et al. 2016;
70 Lhospice et al. 2017; Laffont and Arnoux 2020) and staphylopine is involved in the sensitivity of *S. aureus*
71 to copper intoxication (Hossain et al. 2023). Consistent with this versatility, the *cnt* operon governing
72 staphylopine synthesis, secretion, and metal uptake in *S. aureus* is regulated by both zinc and iron
73 availability (Fojcik et al. 2018). Although well characterized in *S. aureus* and *P. aeruginosa*, nicotianamine-
74 like metallophores are widespread among pathogenic and environmental bacteria (Laffont and Arnoux
75 2020; Morey and Kehl-Fie 2020). Recently, biochemical analyses identified a novel nicotianamine-like
76 metallophore, yersinopine, through *in vitro* assays using purified CntM from *Yersinia pestis*, the agent of
77 flea-borne plague (McFarlane et al. 2018). However, its production *in vivo* and biological role remain
78 unknown.

79 *Y. pestis* emerged within the past 6,000 years from *Yersinia pseudotuberculosis*, an enteropathogen that

80 causes mild enteric infections in humans (Achtman et al. 1999). The mechanisms underlying this
81 emergence remain partially understood but involve the acquisition and loss (through deletion or
82 pseudogenization) of a few genes (Chain et al. 2004; Hinnebusch et al. 2016). Of interest with regard to
83 metal homeostasis, a frameshift mutation in *ureD* abolished the nickel-dependent urease activity of *Y. pestis*
84 (Sebbane et al. 2001). This mutation eliminated urease activity and increased flea infection incidence by
85 reducing bacterial toxicity towards fleas (Chouikha and Hinnebusch 2014). In this context, it is noteworthy
86 that *cntQ* (sometimes called *fiuA* or *fhuD*), encoding the predicted inner membrane importer of yersinopine-
87 metal complexes, is disrupted in *Y. pestis* due to two frameshift mutations relative to *Y. pseudotuberculosis*
88 (Supplementary Figure 1 for sequence alignments of the *cnt* genes; Supplementary Figures 2-4 for the
89 AlphaFold analyses supporting the impairment of the permease; Supplementary Table 1 for the
90 conservation of these two mutations in *Yersinia* species). Furthermore, staphylopine (an epimer of
91 yersinopine) has been linked to urease activity in *S. aureus* (Remy et al. 2013). These observations suggest
92 a possible link between *cntQ* disruption and loss of urease activity in *Y. pestis*. However, *cntQ* is part of the
93 *cntPQRLMI* operon, predicted to govern yersinopine synthesis (*cntLM*) and export (*cntI*), and recovery of
94 yersinopine-metal complexes via an ABC transporter (*cntPQR*) (Figure 1). Altogether, these observations
95 raise the question of whether *Y. pestis* still synthesizes and secretes yersinopine, and if so, whether it
96 contributes to metal uptake in *Y. pestis* and *Y. pseudotuberculosis*.

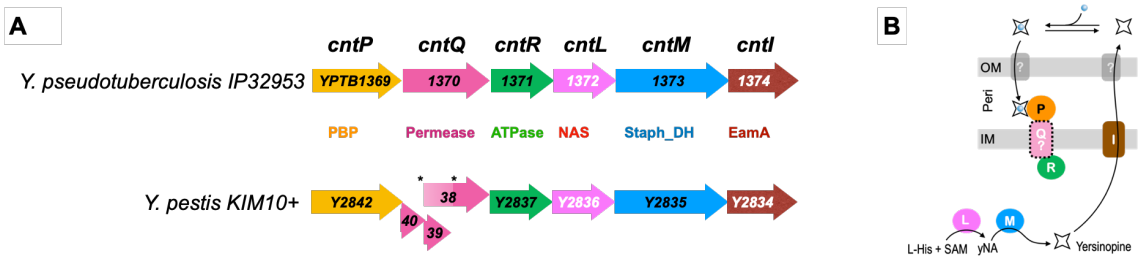

97

98 **Figure 1.** Comparison of the *cnt* operon structure in *Y. pseudotuberculosis* and *Y. pestis*. *A,* Two single-
99 base deletions in the *Y. pestis* genome (indicated by stars) generate frameshift mutations in the *cntQ* gene.
100 The first deletion produces a premature stop codon, leading to ORF Y2840. The second causes two
101 additional ORFs (Y2839 and Y2838) that are frameshifted relative to *Y. pseudotuberculosis cntQ*. Notably,
102 the second deletion restores the reading frame for the last 162 residues, resulting in partial identity between
103 *Y. pestis* CntQ (residues 118–280) and *Y. pseudotuberculosis* CntQ (YPTB1370, residues 190–352). These
104 three predicted ORFs are unlikely to encode a functional permease. Frameshifted region is shown in light
105 color. Other proteins encoded by the operons share 99.3% (CntL), 99.7% (CntP), or 100% (CntR, CntM,
106 and CntI) sequence identity between the two species. *B,* Model of yersinopine biosynthesis, export, and
107 import of yersinopine-metal complexes in the periplasm of *Yersinia* species.

108 **Materials and Methods**

109 ***Bacterial strains, plasmids and culture conditions***

110 Bacterial strains are listed in Supplementary Table 2. Cultures were grown aerobically at 28 °C with shaking
111 in TMH minimal medium. Composition of TMH medium is listed in supplementary Table 3, and ICP-OES
112 metal content is indicated in Supplementary Table 4. Inoculation was performed at 5.10^6 cells/mL into
113 50 mL of medium in sterile 250-mL clear polystyrene bottles (Easy Grip Corning, VWR). Media were
114 prepared with plasticware and sterilized by 0.22-µm filtration to minimize metal contamination. Growth
115 was monitored by measuring OD_{600} over time.

116 ***Mutant construction***

117 *Y. pseudotuberculosis* mutants were generated by allelic exchange using suicide plasmid pDS132
118 derivatives in *E. coli* S17-1λpir, followed by conjugation (Simon et al. 1983) (Supplementary Table 2). *Y.*
119 *pestis* mutants were constructed by Red recombination using plasmid pEP1436 as previously described
120 (Pradel et al. 2014; Dewitte et al. 2020). In both species, antibiotic resistance cassettes were eventually
121 removed by FLP-mediated recombination from plasmid pFLP3, which was subsequently cured by sucrose
122 counter selection. Chromosomal *cnt*::*lacZ* fusions were generated in *Y. pseudotuberculosis* and *Y. pestis* by
123 kanamycin selection following conjugative transfer of suicide plasmids pEP696 or pEP620. The *Y.*
124 *pseudotuberculosis cntPQRLMI* operon was cloned into pEP699 by ExoCET assembly (Wang et al. 2018)
125 and inserted into the mini*Tn*7T-Zeo2 vector pEP1046. Site-specific chromosomal integration was achieved
126 by triparental mating with *E. coli* S17-1λpir strains carrying pEP701 and pTNS3, and verified by PCR.

127 ***Growth curves and doubling time***

128 Overnight cultures were grown aerobically at 28°C in TMH medium using polycarbonate Erlenmeyer
129 flasks. Three independent biological replicates were inoculated at an initial OD_{600} of 0.05 into fresh TMH
130 medium (200 µL) supplemented with various concentrations of EDTA (0–800 µM) in 96-well flat-bottom
131 plates (Corning Costar 3596). Growth was monitored every 15 min for 24 hours at 28°C using a Tecan
132 Spark Microplate Reader under continuous shaking. OD_{600} values were corrected for background
133 absorbance using non-inoculated media. Growth curves were analyzed in RStudio, and doubling times were
134 calculated using the Growthcurver package (Sprouffske and Wagner 2016).

135 ***Genome analysis, protein cloning, expression and purification***

136 The synteny and sequence conservation of *cnt* genes across *Y. pestis* and *Y. pseudotuberculosis* strains were
137 analyzed using the MaGe MicroScope platform (Vallenet et al. 2020). The *cntL* and *cntM* genes (*yptb1372–*
138 *1373*) were amplified from *Y. pseudotuberculosis* 2777 genomic DNA using Q5® High-Fidelity DNA
139 polymerase (New England BioLabs) and cloned into the pET-SUMO vector (Champion™ pET SUMO
140 Protein Expression System, Invitrogen). C-terminal His-tagged proteins were expressed *in E. coli*
141 BL21(DE3) carrying pRARE and purified by nickel affinity chromatography (HisTrap column, GE
142 Healthcare) according to the manufacturer's instructions. Eluted proteins were dialyzed into imidazole-free
143 buffer (20 mM Na_2HPO_4, 300 mM NaCl, 10% glycerol, pH 7.5) and analyzed by SDS-PAGE (NuPAGE
144 10% Bis-Tris gels, Invitrogen).

145 ***Detection of yersinopine by TLC assay***

146 TLC assays were performed as previously described for staphylopine, pseudopaline, and bacillopaline
147 detection (Higuchi et al. 1999; Ghssein et al. 2016; Lhospice et al. 2017; Laffont et al. 2019). Purified CntL
148 and CntM proteins (2.5 µM each) were incubated with carboxyl-[^{14}C]-labeled SAM (2.5 µM), L- or D-
149 histidine (1 mM), NADPH or NADH (10 µM), and pyruvate or α-ketoglutarate (1 mM) in 50 mM HEPES
150 buffer (pH 9) containing 1 mM DTT and 1 mM EDTA. Reactions (100 µL) were carried out for 30 min at
151 28°C and stopped by adding ethanol to 50% (v/v). Samples (10 µL) were spotted onto HPTLC Silica Gel
152 60 plates (Merck) and developed with a phenol:n-butanol:formate:water (12:3:2:3, v/v) solvent system.
153 After drying, plates were exposed to [^{14}C]-sensitive imaging plates (GE Healthcare) for 24 h and scanned
154 with a Typhoon FLA 7000 phosphorimager.

155 ***Sample preparation and detection of yersinopine by HILIC/ESI-MS***

156 For *in vitro* assays, purified CntL and CntM (2.5 µM each) were incubated with SAM (2.5 µM), L-histidine
157 (1 mM), NADPH or NADH (10 µM), and pyruvate or α-ketoglutarate (1 mM) in 50 mM HEPES buffer
158 (pH 9) supplemented with 1 mM DTT and 1 mM EDTA. Reactions were carried out at 28°C for 30 min,
159 then frozen at -80°C until analysis. For extracellular samples, supernatants of *Y. pestis* and *Y.*
160 *pseudotuberculosis* cultures grown for 24 h at 28°C in TMH medium were collected after centrifugation
161 (5,000 × g, 20 min, 4°C), filtered (0.22 µm), and stored at -80°C. Samples were analyzed by hydrophilic
162 interaction liquid chromatography coupled with electrospray ionization mass spectrometry (HILIC/ESI-

163 MS). Separations were performed on a TSKgel Amide-80 column (Tosoh Biosciences) using a linear
164 gradient of acetonitrile and 10 mM ammonium formate (pH 5.5) at a flow rate of 50 µL/min. An Agilent
165 1100 HPLC system coupled to an LTQ Orbitrap Velos mass spectrometer (Thermo Fisher Scientific) was
166 used. Prior to injection, samples were diluted 1:2 with acetonitrile, centrifuged, and injected (7 µl). MS
167 spectra were recalibrated offline using internal standards.

168 ***Analysis of metal concentration by ICP-MS***

169 *Y. pestis* and *Y. pseudotuberculosis* grown in TMH medium under aerobic conditions at 28°C for 24 h were
170 centrifuged (4,000 g, 20 min, 4°C). Bacterial pellets were washed with 20 mM ammonium acetate, dried at
171 50°C for 48 h, and digested with a mixture of 70% HNO_3 and 30% H_2O_2. After heating at 80°C for 3 h,
172 samples were diluted to 2 mL with water and analyzed by inductively coupled plasma mass spectrometry
173 (ICP-MS, Agilent 7500cs) operating in hydrogen collision gas mode.

174 ***Statistical analysis***

175 ICP-MS measurements were performed on two or three independent biological triplicates, collected on
176 different days. For each experiment, metal content was normalized to the corresponding wild-type strain.
177 Statistical analyses were conducted in RStudio (version 4.1.1). Differences between mutant and wild-type
178 strains were assessed using Welch's t-test after normality verification. p-values were adjusted for multiple
179 testing using the Bonferroni method.
180

181 **Results**

182 ***Biochemical evidence that yersinopine is produced by Y. pseudotuberculosis.*** Yersinopine
183 production was previously inferred through biochemical assays of the CntM enzyme from *Y. pestis* under
184 steady-state kinetic conditions (McFarlane et al. 2018), but the full biosynthetic pathway remained
185 incomplete because CntL was not purified. Here, we completed the pathway by characterizing purified
186 recombinant CntL and CntM from *Y. pseudotuberculosis* (Supplementary Figure S5) using multiple
187 biochemical assays. First, we used a ^{14}C-labelled SAM substrate assay to trace the aminobutyrate moiety
188 of SAM in the presence of L-histidine or D-histidine, followed by separation on a TLC plate. This approach
189 demonstrated that CntL indeed specifically uses SAM and L-histidine to generate the yNA intermediate
190 (Figure 2(A)). Building on this result, co-incubation of CntL and CntM with SAM, L-histidine, α-ketoacids,
191 and NAD(P)H showed that CntM utilizes NADPH to reductively condense yNA with pyruvate, yielding
192 yersinopine (Figure 2(B)). HILIC/ESI-MS analysis further validated the use of L-histidine (Figure 2(C))
193 and pyruvate (Figure 2(D)) by CntL and CntM, respectively. Collectively, our results demonstrate that CntL
194 and CntM catalyze the formation of yersinopine according to the reaction pathway shown in Figure 2E.
195 Given the 99.3% and 100% sequence identity of CntL and CntM between *Y. pseudotuberculosis* and *Y.*
196 *pestis*, it is highly likely that *Y. pestis* produces an identical metallophore, namely yersinopine.

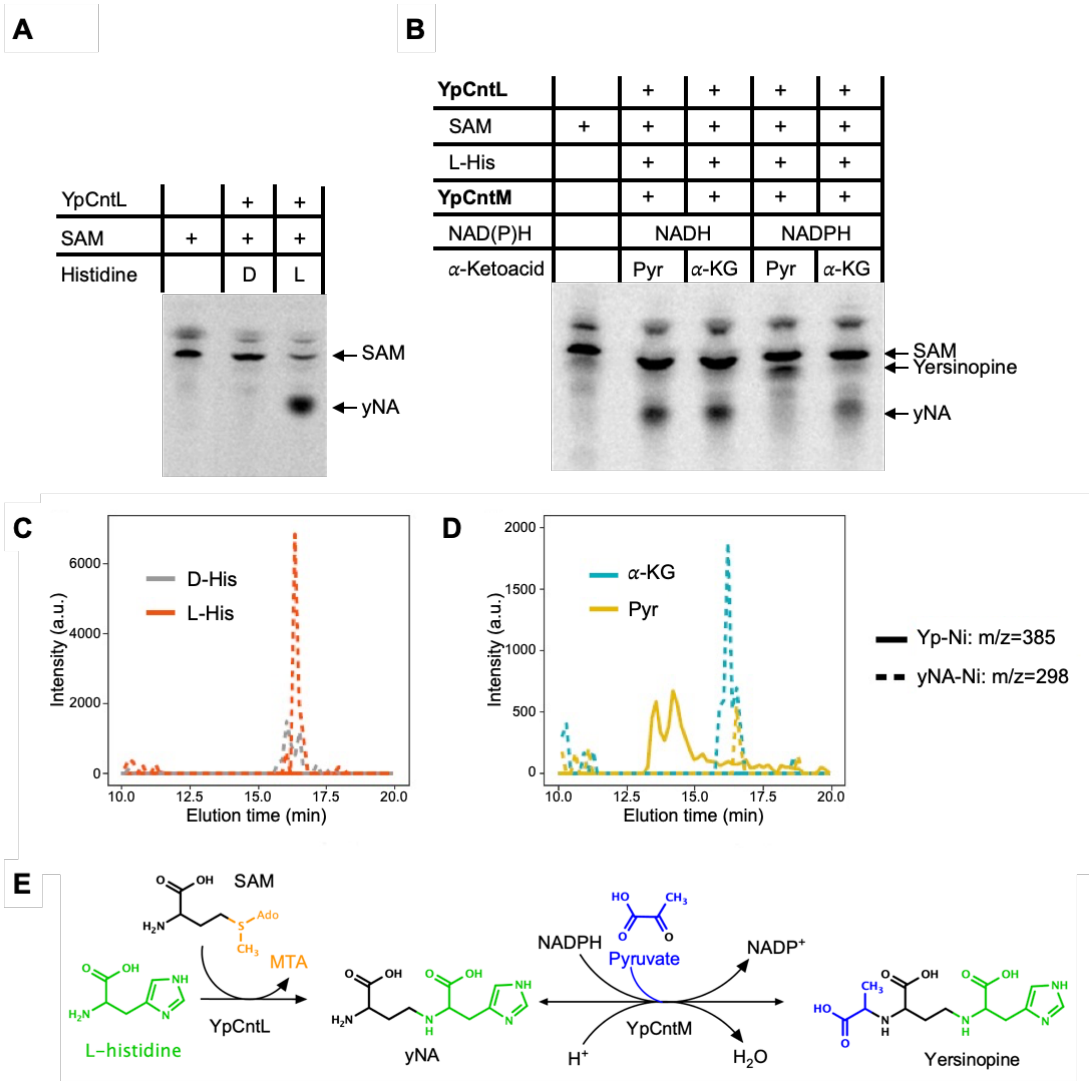

Figure 2. *In vitro* selectivity of CntL and CntM. *A,* Radiogram showing the activity of CntL after incubation with ^{14}C-SAM and either L- or D-histidine. *B,* Radiogram after co-incubation of CntL (with ^{14}C-SAM and L-histidine) and CntM with pyruvate or α-ketoglutarate (α-KG) and NAD(P)H. *C,* HILIC/ESI-MS detection of the yNA-nickel complex (dashed line) after incubation of CntL with SAM and either L- or D-histidine. *D*, HILIC/ESI-MS detection of yNA-nickel (dashed line) or yersinopine-nickel (solid line) complexes after co-incubation of CntL (with SAM and L-histidine) and CntM (with NADPH and either pyruvate or α-KG). *E,* Schematic representation of the overall yersinopine biosynthetic pathway.

Yersinopine is produced and exported by both Y. pseudotuberculosis and Y. pestis. After establishing the roles of CntL and CntM in yersinopine biosynthesis, and inferring that CntI mediates its export across the inner membrane (Lhospice et al. 2017; McFarlane et al. 2018; Laffont et al. 2019), we next investigated whether yersinopine is produced and secreted by both *Y. pestis* and *Y. pseudotuberculosis*. To this end, we quantified yersinopine in the extracellular fractions of both bacteria grown in TMH medium

211 using HILIC coupled with ESI-MS (Figure 3). Yersinopine was detected complexed with multiple divalent
212 metals, predominantly zinc, and to a lesser extent copper, nickel, and cobalt. This distribution might be a
213 proxy for the higher affinity of yersinopine for zinc under these conditions. Iron(II)-yersinopine complexes
214 were not observed, likely due to oxidation under aerobic conditions. Metal-yersinopine complexes were
215 detected in the supernatants of both species, although the abundance was lower in *Y. pestis*, suggesting a
216 reduced extracellular concentration compared to *Y. pseudotuberculosis*. Collectively, these results
217 demonstrate that both species produce and secrete yersinopine. Moreover, they reveal that the
218 pseudogenization of *cntQ* in *Y. pestis* does not impair the operon's ability to govern yersinopine
219 biosynthesis and secretion.

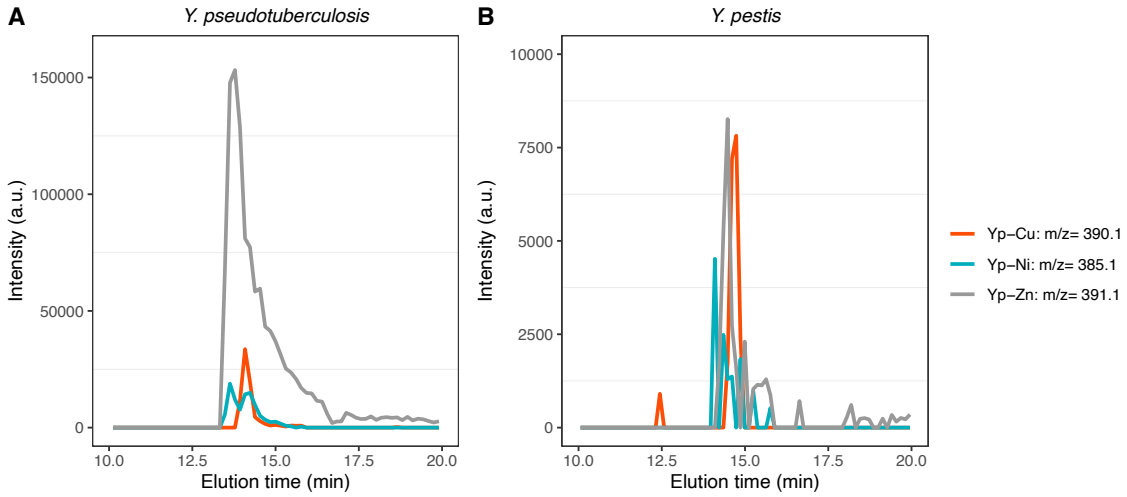

220

221 **Figure 3.** *In vivo* production and secretion of yersinopine by *Y. pseudotuberculosis* and *Y. pestis*.
222 HILIC/ESI-MS detection of divalent yersinopine-metal complexes in culture supernatants of *Y.*
223 *pseudotuberculosis* (A) and *Y. pestis* (B).
224

225 ***The cnt operon is repressed by Zur in both Y. pseudotuberculosis and Y. pestis.*** Previous
226 studies of the Zur regulon in *Y. pestis* (Li et al. 2009; Desrosiers et al. 2010) and *Y. pseudotuberculosis* (Gu
227 et al. 2024) revealed strong upregulation of *cntP* in Zur-deficient strains (227-fold in *Y. pestis*, 9-fold in *Y.*
228 *pseudotuberculosis*), along with induction of downstream operon genes (ranging from 45-fold to 6-fold
229 depending on the gene). However, at that time, the function of the *cnt* system remained unclear. Although
230 Zur was also implicated in zinc homeostasis and oxidative stress defense in *Y. pseudotuberculosis* (Wang
231 et al. 2016), the role of the *cnt* system itself was not addressed. Given that both *Y. pseudotuberculosis* and
232 *Y. pestis* produce yersinopine, we next investigated whether the *cnt* operon is subject to Zur regulation. To

233 test this, we inserted a *lacZ* transcriptional reporter downstream of the *cnt* promoter in Zur^+ and Zur^- strains
234 of both species. As expected, promoter activity was repressed in Zur^+ strains and derepressed in Zur^-
235 mutants grown in rich medium (Supplementary Figure 6). These findings confirm that Zur represses the
236 *cnt* operon in both *Y. pestis* and *Y. pseudotuberculosis* in zinc-repleted conditions.

237 ***Yersinopine mediates distinctive strategies of metal uptake in Y. pseudotuberculosis***
238 ***and Y. pestis.*** Since the *cnt* operon is repressed by Zur and involved in yersinopine production and
239 secretion, we next examined the impact of *cnt* deletions on metal accumulation. To explore the role of the
240 *cnt* operon, we generated mutants in both species, including a strain lacking *cntQ* with a polar effect,
241 abolishing yersinopine production (Δ*cntQ(RLMI)*), and a strain lacking *cntLMI* (Δ*cntLMI*; see Methods).
242 In *Y. pseudotuberculosis*, we also generated a non-polar Δ*cntQ* mutant to mimic the genetic configuration
243 of *Y. pestis*. When TMH medium was supplemented with EDTA (a metal chelator commonly used to trigger
244 metal deficiency) the growth rate of the *Y. pseudotuberculosis* wild-type strain increased, whereas *cnt*
245 mutants exhibited reduced growth (Supplementary Figure 7). This suggests that the *cnt* operon provides a
246 growth advantage under these metal-limited conditions. However, in order to compare wild-type and
247 mutant strains across both species, we grew them in TMH medium without EDTA (conditions in which we
248 established yersinopine secretion by both species) and measured intracellular metal content by inductively
249 coupled plasma mass spectrometry (ICP-MS).

250 In *Y. pseudotuberculosis*, loss of the yersinopine biosynthetic genes (Δ*cntQ(RLMI)* and Δ*cntLMI*) led to a
251 slight but significant reduction in intracellular iron content (-27.6%, $p = 3.7\times10^{-5}$ and -31.1%, $p = 4.5\times10^{-}$
252 ^{3}, respectively), without affecting zinc or other metals (Figure 4(A)). Complementation restored iron to
253 wild-type levels. By contrast, in *Y. pestis,* iron content was unchanged, but zinc levels decreased
254 significantly in both Δ*cntQ(RLMI)* and Δ*cntLMI* mutants (-47.3%, $p = 6.2\times10^{-3}$ and -50.9%, $p = 1.9\times10^{-2}$),
255 while cobalt levels rose substantially (+176.4%, $p=2.8\times10^{-6}$ and +182.2%) (Figure 4(B)).

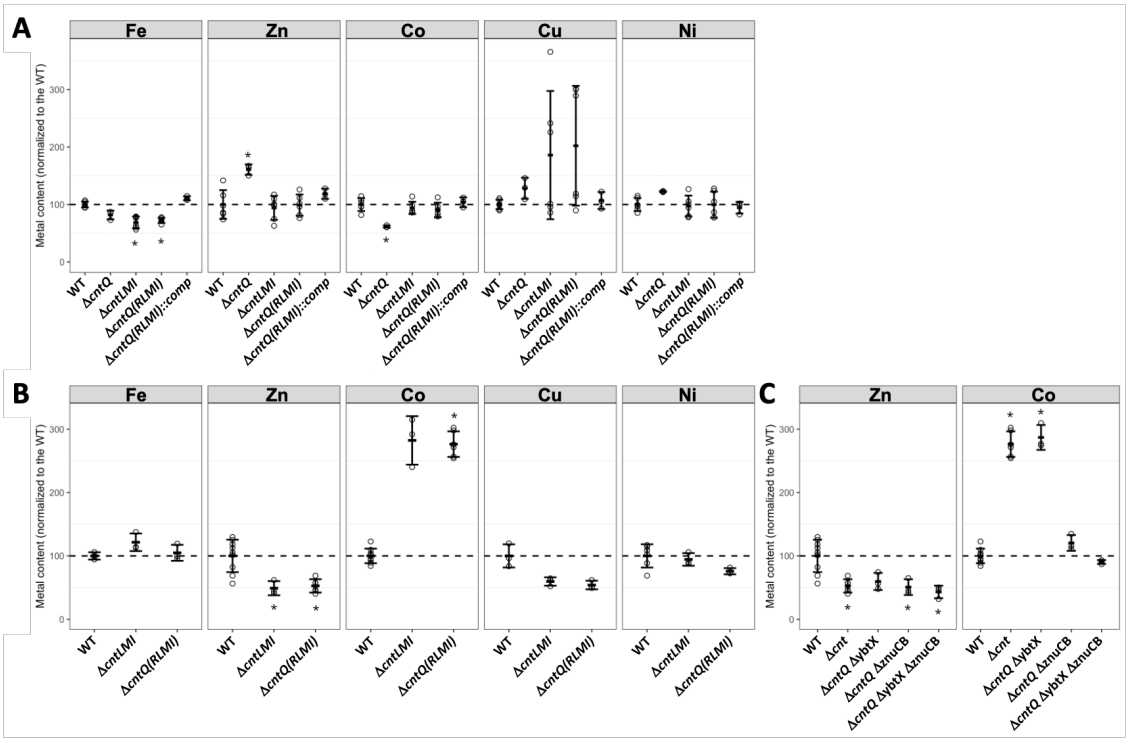

Figure 4. Intracellular metal content in *Y. pseudotuberculosis* and *Y. pestis* strains. *A,* ICP-MS quantification of intracellular metals in *Y. pseudotuberculosis* wild-type (WT) and *cnt* mutants. *B,* ICP-MS quantification of intracellular metals in *Y. pestis* WT and *cnt* mutants. *C,* Intracellular zinc and cobalt levels in *Y. pestis* WT and strains lacking the Cnt system alone or combined with deletions of the yersiniabactin transporter (YbtX) and/or the ZnuABC zinc importer. Data are from 1 to 3 independent triplicates (total n= 3-9). Asterisks (*) indicate significant differences relative to WT (Welch's t-test with Bonferroni correction; $p < 0.05$).

To further explore zinc and cobalt uptake, we analyzed *Y. pestis Δcnt* mutants additionally lacking either the putative yersiniabactin importer YbtX (which mediates yersiniabactin-zinc uptake) (Price et al. 2021), the Znu zinc uptake system, or both (Figure 4(C)). Compared to the yersinopine-deficient mutant, intracellular zinc concentrations did not decrease further in the double and triple mutants, indicating that unidentified zinc uptake mechanisms remain active. In contrast, cobalt accumulation returned to wild-type values in the Δ*cnt* Δ*znu* and Δ*cnt* Δ*ybtX* Δ*znu* mutants, but remained elevated in mutants lacking only *cnt* or both *cnt* and *ybtX*. These findings suggest that in the absence of yersinopine, cobalt can be imported through Znu, whereas the presence of yersinopine may inhibit cobalt uptake via Znu in *Y. pestis*.

Deletion of cntQ in Y. pseudotuberculosis mimics the evolutionary shift in metal-

274 ***uptake specificity.*** Our findings suggest that during the emergence of *Y. pestis* from *Y.*
275 *pseudotuberculosis*, pseudogenization of *cntQ* reshaped metal-uptake specificity from iron to zinc. To
276 directly test this hypothesis, we deleted *cntQ* in *Y. pseudotuberculosis*. Strikingly, the reduction in
277 intracellular iron observed in yersinopine-deficient strains was no longer detectable. Instead, *cntQ* deletion
278 triggered a significant rise in zinc (+60.8%, $p = 2.5\times10^{-2}$) and a concomitant fall in cobalt (-38.4%, $p =$
279 5.8×10^{-3}) (Figure 4(A)). This shift recapitulates the metal-uptake profile of wild-type *Y. pestis*, where the
280 Cnt system promotes zinc acquisition while restricting cobalt accumulation. Thus, production of
281 yersinopine combined with a defective yersinopine-metal complex inner membrane importer rewires metal
282 transport toward zinc uptake and limits cobalt entry via the Znu system, closely mirroring the transport
283 dynamics observed in *Y. pestis*.
284

285 **Discussion**

286 A functional yersinopine-mediated metal uptake system (*cntPQRLMI*) was predicted in *Y.*
287 *pseudotuberculosis*, but the presence of a frameshift mutation in the *cntQ* permease gene suggested that
288 this system was non-functional in *Y. pestis* (Forman et al. 2010). Here, we demonstrate that yersinopine is
289 produced and secreted by both *Y. pseudotuberculosis* and *Y. pestis* when grown in the same low-zinc
290 medium, indicating that production and export are preserved despite the inactivation of *cntQ* in *Y. pestis*.
291 These findings suggest that the *cnt* operon retains some function despite the pseudogenization of *cntQ*. This
292 is further supported by transcriptomic data showing that the *Y. pestis cnt* operon is controlled by the Zur
293 repressor (Li et al. 2009) and is strongly induced during pneumonic infection (Perry et al. 2015). Therefore,
294 an important question that arises is the role of yersinopine in the context of either a fully functional Cnt
295 system (*Y. pseudotuberculosis*) or a system lacking the ABC importer permease (*Y. pestis*).

296 Our data suggest that the Cnt system is not involved in nickel uptake in *Y. pestis* and *Y. pseudotuberculosis*,
297 in contrast to findings in *P. aeruginosa* (Mastropasqua et al. 2017; Lhospice et al. 2017) and *S. aureus*
298 (Remy et al. 2013). Unexpectedly, our results indicate that the presence or absence of the CntQ permease
299 influences metal-uptake specificity in *Yersinia*, shifting from an iron uptake system when CntQ is present
300 (*Y. pseudotuberculosis*) to a zinc uptake system when CntQ is absent (*Y. pestis*). The main limitation of our
301 study is that we do not differentiate between compartmentalization of metal accumulation, *i.e.* this could
302 occur in the periplasm as well as in the cytoplasm. To our knowledge, this represents a unique case where
303 pseudogenization of a permease within an ABC transporter leads to a shift in substrate specificity, even if
304 metals may accumulate in different compartments of the cell. Interestingly, a frameshift mutation in the
305 *iucA* gene, which encodes a key enzyme in aerobactin siderophore biosynthesis, has also been identified in
306 *Y. pestis*. However, the bacterium remains capable of utilizing aerobactin-iron complexes for iron uptake,
307 presumably through piracy of aerobactin produced by other bacteria in its biotope (Forman et al. 2007).
308 The extent to which our finding that the yersinopine system of *Y. pestis* is involved in zinc homeostasis *in*
309 *vitro* translates to host-associated or other environmentally relevant conditions remains to be evaluated.

310 Functional studies of the Znu system in *Y. pestis* indicated that it is not required for virulence, suggesting
311 the existence of additional zinc-uptake mechanisms (Desrosiers et al. 2010). Among these, yersiniabactin-
312 mediated zinc acquisition was later recognized (Price et al. 2021). Our findings further expand this
313 understanding by revealing that the *cnt* operon also plays a critical role in zinc uptake. While the entire

314 operon appears essential, the route of zinc entry in the cell is unknown and the specific role of the
315 periplasmic protein CntP remains uncertain. It may either be rerouted to an alternative transporter or act
316 indirectly, for instance by chelating a yersinopine-metal complex. Consistent with this, the very likely
317 impairment of CntQ in *Y. pestis* supports the hypothesis that yersinopine functions independently of CntP
318 or CntP-R. In this context, analyzing mutants lacking *cntPQR* in both *Y. pestis* and *Y. pseudotuberculosis*
319 would be particularly informative to clarify CntP's role in metal acquisition.

320 The increased intracellular cobalt accumulation in *Y. pestis* upon inactivation of the *cnt* operon was
321 unexpected. However, we found that this increase was correlated with the presence of a functional Znu
322 system, as the absence of both Cnt and Znu systems restored intracellular cobalt levels to wild-type values.
323 This interplay between the Znu and Cnt systems could be explained by the ability of yersinopine to form a
324 complex with cobalt in the periplasmic space, thereby preventing cobalt entry into the cytoplasm via the
325 Znu system. A connection between Znu and cobalt transport has been previously described in *P. aeruginosa*
326 (Pederick et al. 2015; Mastropasqua et al. 2017), where cobalt uptake was found to increase in a mutant
327 lacking the ZnuABC transporter, suggesting a zinc-regulated cobalt uptake mechanism. Although the
328 mechanisms differ, both our findings and prior studies underscore the frequent cross-talk between zinc and
329 cobalt uptake systems. A model summarizing zinc and cobalt import via the Cnt and Znu systems in both
330 *Y. pseudotuberculosis* and *Y. pestis* is presented in Figure 5. This model also illustrates how small genetic
331 changes can significantly alter bacterial physiology, potentially influencing pathogen evolution and
332 adaptation.

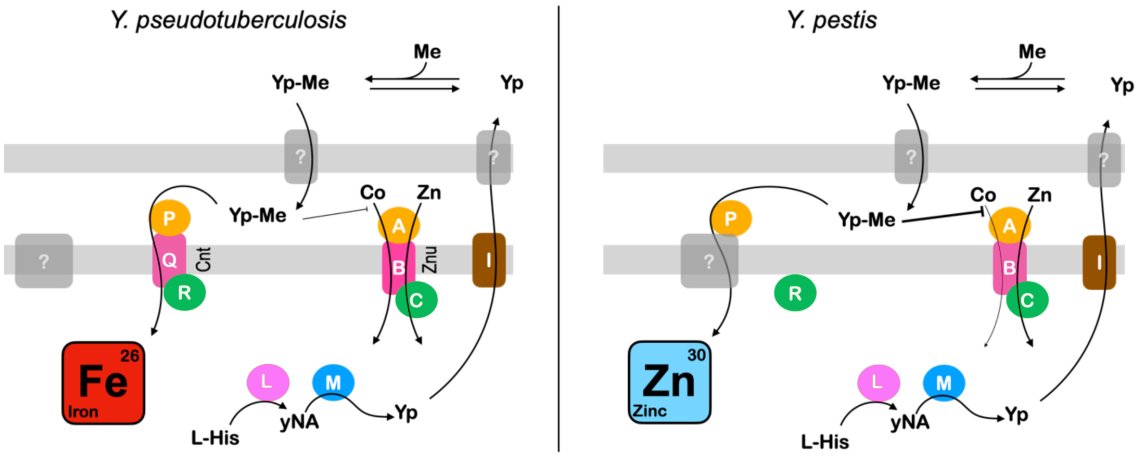

333

334 **Figure 5.** Comparative model of metal uptake through the Cnt and Znu systems in *Y. pseudotuberculosis*
335 and *Y. pestis*. In *Y. pseudotuberculosis*, yersinopine-metal complexes in the periplasm facilitate iron uptake,
336 presumably via the CntPQR ABC transporter encoded by the *cnt* operon. In *Y. pestis*, the absence of the

CntQ permease, due to a frameshift mutation, alters metal homeostasis. Zinc import via the Cnt system appears to occur through rerouting of the yersinopine-zinc complex to an unknown inner membrane transporter (indicated by "?"), potentially involving CntP in the periplasm. In both *Yersinia* species, two additional unknown steps at the outer-membrane are proposed, including the export of yersinopine to the extracellular space and the import of yersinopine-metal complexes into the periplasm.

342 **References**

343 Achtman M, Zurth K, Morelli G, et al (1999) *Yersinia pestis*, the cause of plague, is a
344 recently emerged clone of *Yersinia pseudotuberculosis*. Proceedings of the
345 National Academy of Sciences 96:14043–14048.
346 https://doi.org/10.1073/pnas.96.24.14043

347 Bibi-Triki S, Li de la Sierra-Gallay I, Lazar N, et al (2014) Functional and Structural
348 Analysis of HicA3-HicB3, a Novel Toxin-Antitoxin System of *Yersinia pestis*.
349 Journal of Bacteriology 196:3712–3723. https://doi.org/10.1128/JB.01932-14

350 Chain PSG, Carniel E, Larimer FW, et al (2004) Insights into the evolution of *Yersinia*
351 *pestis* through whole-genome comparison with *Yersinia pseudotuberculosis*.
352 Proc Natl Acad Sci U S A 101:13826–13831.
353 https://doi.org/10.1073/pnas.0404012101

354 Chandrangsu P, Rensing C, Helmann JD (2017) Metal homeostasis and resistance in
355 bacteria. Nat Rev Microbiol 15:338–350.
356 https://doi.org/10.1038/nrmicro.2017.15

357 Choi K-H, Gaynor JB, White KG, et al (2005) A Tn7-based broad-range bacterial
358 cloning and expression system. Nat Methods 2:443–448.
359 https://doi.org/10.1038/nmeth765

360 Chouikha I, Hinnebusch BJ (2014) Silencing urease: a key evolutionary step that
361 facilitated the adaptation of *Yersinia pestis* to the flea-borne transmission route.
362 Proc Natl Acad Sci U S A 111:18709–18714.
363 https://doi.org/10.1073/pnas.1413209111

364 Datsenko KA, Wanner BL (2000) One-step inactivation of chromosomal genes in
365 *Escherichia coli* K-12 using PCR products. Proceedings of the National
366 Academy of Sciences 97:6640–6645. https://doi.org/10.1073/pnas.120163297

367 Desrosiers DC, Bearden SW, Mier I, et al (2010) Znu Is the Predominant Zinc Importer
368 in *Yersinia pestis* during In Vitro Growth but Is Not Essential for Virulence.
369 Infect Immun 78:5163–5177. https://doi.org/10.1128/IAI.00732-10

370 Dewitte A, Bouvenot T, Pierre F, et al (2020) A refined model of how *Yersinia pestis*
371 produces a transmissible infection in its flea vector. PLOS Pathogens
372 16:e1008440. https://doi.org/10.1371/journal.ppat.1008440

373 Fojcik C, Arnoux P, Ouerdane L, et al (2018) Independent and cooperative regulation of
374 staphylopine biosynthesis and trafficking by Fur and Zur. Mol Microbiol
375 108:159–177. https://doi.org/10.1111/mmi.13927

376 Forman S, Nagiec MJ, Abney J, et al (2007) Analysis of the aerobactin and ferric
377 hydroxamate uptake systems of *Yersinia pestis*. Microbiology (Reading)
378 153:2332–2341. https://doi.org/10.1099/mic.0.2006/004275-0

379 Forman S, Paulley JT, Fetherston JD, et al (2010) Yersinia ironomics: comparison of
380 iron transporters among *Yersinia pestis* biotypes and its nearest neighbor,

Yersinia pseudotuberculosis. Biometals 23:275–294. https://doi.org/10.1007/s10534-009-9286-4

Ghssein G, Brutesco C, Ouerdane L, et al (2016) Biosynthesis of a broad-spectrum nicotianamine-like metallophore in *Staphylococcus aureus*. Science 352:1105–1109. https://doi.org/10.1126/science.aaf1018

Grim KP, San Francisco B, Radin JN, et al (2017) The Metallophore Staphylopine Enables *Staphylococcus aureus* To Compete with the Host for Zinc and Overcome Nutritional Immunity. MBio 8:. https://doi.org/10.1128/mBio.01281-17

Gu Y, Liu Y, Mao W, et al (2024) Functional versatility of Zur in metal homeostasis, motility, biofilm formation, and stress resistance in *Yersinia pseudotuberculosis*. Microbiology Spectrum 12:e03756-23. https://doi.org/10.1128/spectrum.03756-23

Higuchi K, Suzuki K, Nakanishi H, et al (1999) Cloning of nicotianamine synthase genes, novel genes involved in the biosynthesis of phytosiderophores. Plant Physiology 119:471–480

Hinnebusch BJ, Chouikha I, Sun Y-C (2016) Ecological Opportunity, Evolution, and the Emergence of Flea-Borne Plague. Infection and Immunity 84:1932–1940. https://doi.org/10.1128/IAI.00188-16

Hood MI, Skaar EP (2012) Nutritional immunity: transition metals at the pathogen–host interface. Nature Reviews Microbiology 10:525–537. https://doi.org/10.1038/nrmicro2836

Hossain S, Morey JR, Neville SL, et al (2023) Host subversion of bacterial metallophore usage drives copper intoxication. mBio 14:e0135023. https://doi.org/10.1128/mbio.01350-23

Laffont C, Arnoux P (2020) The ancient roots of nicotianamine: diversity, role, regulation and evolution of nicotianamine-like metallophores. Metallomics 12:1480–1493. https://doi.org/10.1039/d0mt00150c

Laffont C, Brutesco C, Hajjar C, et al (2019) Simple rules govern the diversity of bacterial nicotianamine-like metallophores. Biochem J 476:2221–2233. https://doi.org/10.1042/BCJ20190384

Lhospice S, Gomez NO, Ouerdane L, et al (2017) *Pseudomonas aeruginosa* zinc uptake in chelating environment is primarily mediated by the metallophore pseudopaline. Sci Rep 7:17132. https://doi.org/10.1038/s41598-017-16765-9

Li Y, Qiu Y, Gao H, et al (2009) Characterization of Zur-dependent genes and direct Zur targets in *Yersinia pestis*. BMC Microbiology 9:128. https://doi.org/10.1186/1471-2180-9-128

Ma Z, Jacobsen FE, Giedroc DP (2009) Coordination Chemistry of Bacterial Metal Transport and Sensing. Chemical Reviews 109:4644–4681. https://doi.org/10.1021/cr900077w

421 Mastropasqua MC, D'Orazio M, Cerasi M, et al (2017) Growth of *Pseudomonas*
422 *aeruginosa* in zinc poor environments is promoted by a nicotianamine-related
423 metallophore. Mol Microbiol 106:543–561. https://doi.org/10.1111/mmi.13834

424 McFarlane JS, Davis CL, Lamb AL (2018) Staphylopine, pseudopaline, and yersinopine
425 dehydrogenases: A structural and kinetic analysis of a new functional class of
426 opine dehydrogenase. J Biol Chem 293:8009–8019.
427 https://doi.org/10.1074/jbc.RA118.002007

428 Morey JR, Kehl-Fie TE (2020) Bioinformatic Mapping of Opine-Like Zincophore
429 Biosynthesis in Bacteria. mSystems 5:e00554-20.
430 https://doi.org/10.1128/mSystems.00554-20

431 Nelson CE, Huang W, Zygiel EM, et al (2021) The Human Innate Immune Protein
432 Calprotectin Elicits a Multimetal Starvation Response in *Pseudomonas*
433 *aeruginosa*. Microbiology Spectrum 9:e00519-21.
434 https://doi.org/10.1128/Spectrum.00519-21

435 Pederick VG, Eijkelkamp BA, Begg SL, et al (2015) ZnuA and zinc homeostasis in
436 Pseudomonas aeruginosa. Scientific Reports 5:13139.
437 https://doi.org/10.1038/srep13139

438 Perry RD, Bobrov AG, Fetherston JD (2015) The Role of Transition Metal Transporters
439 for Iron, Zinc, Manganese, and Copper in the Pathogenesis of *Yersinia pestis*.
440 Metallomics 7:965–978. https://doi.org/10.1039/c4mt00332b

441 Philippe N, Alcaraz J-P, Coursange E, et al (2004) Improvement of pCVD442, a suicide
442 plasmid for gene allele exchange in bacteria. Plasmid 51:246–255.
443 https://doi.org/10.1016/j.plasmid.2004.02.003

444 Pradel E, Lemaître N, Merchez M, et al (2014) New Insights into How *Yersinia pestis*
445 Adapts to Its Mammalian Host during Bubonic Plague. PLoS Pathogens
446 10:e1004029. https://doi.org/10.1371/journal.ppat.1004029

447 Price SL, Vadyvaloo V, DeMarco JK, et al (2021) Yersiniabactin contributes to
448 overcoming zinc restriction during *Yersinia pestis* infection of mammalian and
449 insect hosts. Proceedings of the National Academy of Sciences
450 118:e2104073118. https://doi.org/10.1073/pnas.2104073118

451 Remy L, Carrière M, Derré-Bobillot A, et al (2013) The *Staphylococcus aureus* Opp1
452 ABC transporter imports nickel and cobalt in zinc-depleted conditions and
453 contributes to virulence. Molecular Microbiology 87:730–743.
454 https://doi.org/10.1111/mmi.12126

455 Rose RE (1988) The nucleotide sequence of pACYC177. Nucleic Acids Research
456 16:356. https://doi.org/10.1093/nar/16.1.356

457 Sebbane F, Devalckenaere A, Foulon J, et al (2001) Silencing and reactivation of urease
458 in *Yersinia pestis* is determined by one G residue at a specific position in the
459 ureD gene. Infect Immun 69:170–176. https://doi.org/10.1128/IAI.69.1.170-
460 176.2001

461 Simon R, Priefer U, Pühler A (1983) A Broad Host Range Mobilization System for In
462 Vivo Genetic Engineering: Transposon Mutagenesis in Gram Negative Bacteria.
463 Nat Biotechnol 1:784–791. https://doi.org/10.1038/nbt1183-784

464 Sprouffske K, Wagner A (2016) Growthcurver: an R package for obtaining
465 interpretable metrics from microbial growth curves. BMC Bioinformatics
466 17:172. https://doi.org/10.1186/s12859-016-1016-7

467 Vallenet D, Calteau A, Dubois M, et al (2020) MicroScope: an integrated platform for
468 the annotation and exploration of microbial gene functions through genomic,
469 pangenomic and metabolic comparative analysis. Nucleic Acids Research
470 48:D579–D589. https://doi.org/10.1093/nar/gkz926

471 Wang H, Li Z, Jia R, et al (2018) ExoCET: exonuclease in vitro assembly combined
472 with RecET recombination for highly efficient direct DNA cloning from
473 complex genomes. Nucleic Acids Res 46:e28.
474 https://doi.org/10.1093/nar/gkx1249

475 Wang T, Yang X, Gao F, et al (2016) Zinc acquisition via ZnuABC in *Yersinia*
476 *pseudotuberculosis* facilitates resistance to oxidative stress. Ann Microbiol
477 66:1189–1197. https://doi.org/10.1007/s13213-016-1205-7

478 Weinberg ED (1975) Nutritional Immunity: Host's Attempt to Withhold Iron From
479 Microbial Invaders. JAMA 231:39–41.
480 https://doi.org/10.1001/jama.1975.03240130021018

481 Zygiel EM, Nolan EM (2018) Transition Metal Sequestration by the Host-Defense
482 Protein Calprotectin. Annual Review of Biochemistry 87:621–643.
483 https://doi.org/10.1146/annurev-biochem-062917-012312

484

Supplemental material:

CntP

```
YPTB1369-CntP/1-378    1 LIHYNITIKSTRISFMLLRIFWSLCLWWGISSSALAEIHLKDVDGREVTLAAPAQRVYIGFYYEDFLAINGPDSYQHVVAFSKSDWSLRT  90
Y2842-CntP/1-378       1 LIHYNITIKSTRISFMLLRIFWSLCLWWGISSSALAEIHLKDVDGREVTLAAPAQRVYIGFYYEDFLAINGPDSYQHVVAFSKSDWSLRT  90

YPTB1369-CntP/1-378   91 SQWPRYQAALRRLSQLVDVGSLYNQSFDFERLLATRPDLLILAKWQLEGFANYLPVLQQLSIPYVVVDFNQGEDAKLTSIRVMGQALGHG 180
Y2842-CntP/1-378      91 SQWPRYQAALRRLSQLVDVGSLYNQSFDFERLLATRPDLLILAKWQLEGFANYLPVLQQLSIPYVVVDFNQGEDAKLTSIRVMGQALGHG 180

YPTB1369-CntP/1-378  181 ERAERLAIAYQQGIADIRRRITQANLPSPKTYIELGDKGPGEYSSSYGTSIWGPLLQQAGANNIATGVVTTPSPLRAEYVLSQKPEVIFL 270
Y2842-CntP/1-378     181 ERAERLAIAYQQGIADIRRRITQANLPSPKTYIELGDKGPGEYSSSYGSSIWGPLLQQAGANNIATGVVTTPSPLRAEYVLSQKPEVIFL 270

YPTB1369-CntP/1-378  271 AGGDWPKMPNAVSMGFGAKPETLQQSMTQYAQRPGWSQFPAIKQTRFYALYHGGVRTLYDYIFVQFVAKALFPSAFEDVNPQRNLETFYE 360
Y2842-CntP/1-378     271 AGGDWPKMPNAVSMGFGAKPETLQQSMTQYAQRPGWSQFPAIKQTRFYALYHGGVRTLYDYIFVQFVAKALFPSAFEDVNPQHNLETFYE 360

YPTB1369-CntP/1-378  361 EYLPIKADGVFMQQWQGE                                                                          378
Y2842-CntP/1-378     361 EYLPIKADGVFMQQWQGE                                                                          378
```

CntQ

```
YPTB1370-CntQ/1-352    1 -----MATFLEPLTQGRQFFQQLHLRRGLFTLALIGSLLAAMVIDLATGAANLSPLDVLRLFLVDSSQHDELHQII---FWSIRLPMTLT  82
Y2838-CntQ1/1-130                                                                                          LPMTLT   6
Y2839-CntQ2/1-280      1 ----LVHSFADDVN-----------RRGGGREFGFGWLVDANRTGESVSQS---------LYLGDFSRGRIWCRIIDHHWLQRGGSLVIR  66
Y2840-CntQ3/1-83       1 MAGRIMATFLEPITQGRQSFQQLHLRRGLFTLALIGSLLAAMVIDLATGAANLSPLDVLRLFLVDSSQHDELHQII--------------  76

YPTB1370-CntQ/1-352   83 AVVVGASLGLAGLLMQTVLANPLASPYTLGISAAAGFGAALSIITGFSVGGVLSLGTPLLASLMALLACLPIYFMGQRQGMTPQILVLSG 172
Y2838-CntQ1/1-130      7 AVVVGASLGLAGLLMQTVLANPLASPYTLGISAAAGFGAALSIITGFSVGGVLSLGTPLLASLMALLACLPIYFLGQRQGMTPQILVLSG  96
Y2839-CntQ2/1-280     67 HPIIGFTDGITGLPAH-LLSGPTAGDDTANSGVERHCGAVL-------------------------------LPVVAITH------------ 114
Y2840-CntQ3/1-83      77 ------------------------------------------FG-------------------------------------------------  78

YPTB1370-CntQ/1-352  173 IVVLFFFQSLQSLMLFLASPEAMQQIVFWLFGSLLKANMQGVLMTGSVLACSLVICLQQAWRLTALSAGEEQALGLGINVSALRKLAFLL 262
Y2838-CntQ1/1-130     97 IVVLFFFQSLQSLMLFR-------------------------------------------------------------------------- 113
Y2839-CntQ2/1-280    115 --------------VISASPEAMQQIVFWLFGSLLKANMQGVLMTGSVLACSLVICLQQAWRLTALSAGEEQALGLGINVSALRKLAFLL 190
Y2840-CntQ3/1-83         ------------------------------------------------------------------------------------------

YPTB1370-CntQ/1-352  263 ATLLTAASVSFVGTIGFIGLVAPHFARMLVGEDQRYLIGISALCGSLLLVLASIISKLILPNGVVPIGIIIALIGVPVLFYFVTKQVKRA 352
Y2838-CntQ1/1-130    114 ----------------------PHQKRC-----NKLYSGCLAAC------------------------------------------------ 130
Y2839-CntQ2/1-280    191 ATLLTAASVSFVGTIGFIGLVAPHFARMLVGEDQRYLIGISALCGSLLLVLASIISKLILPNGVVPIGIIIALIGVPVLFYFVTKQVKRA 280
Y2840-CntQ3/1-83      79 ----------------------PFVCR-------------------------------------------------------------- 83
```

CntR

```
YPTB1371-CntR/1-261    1 MTQLTLKHVGVTLHKRPLLTDISLTWPAAQVSGIIGPNGAGKSTLLKAINHMVPITGQIEYQQCPLNTRVTRIAYVSQLNRSDSALTVFE  90
Y2837-CntR/1-261       1 MTQLTLKHVGVTLHKRPLLTDISLTWPAAQVSGIIGPNGAGKSTLLKAINHMVPITGQIEYQQCPLNTRVTRIAYVSQLNRSDSALTVFE  90

YPTB1371-CntR/1-261   91 MVLLGKVRQLSWRVSPAQIDAVEQVLAECGISSLANQVFNSLSGGQRQLVMLAQAFIAQPQIILLDEPTSALDIHHQLRVLQKIVDYSKR 180
Y2837-CntR/1-261      91 MVLLGKVRQLSWRVSPAQIDAVEQVLAECGISSLANQVFNSLSGGQRQLVMLAQAFIAQPQIILLDEPTSALDIHHQLRVLQKIVDYSKR 180

YPTB1371-CntR/1-261  181 HQCTTLMVIHDLGLALRFCQTLTLIHRGNVACHGAAHQVIADPMMSTVFGVGIESGTSPLGYRYLLPTQFLPTHGEKICIR           261
Y2837-CntR/1-261     181 HQCTTLMVIHDLGLALRFCQTLTLIHRGNVACHGAAHQVIADPMMSTVFGVGIESGTSPLGYRYLLPTQFLPTHGEKICIR           261
```

CntL

```
YPTB1372-CntL/1-265    1 MYTLMKADVLAQLAGLQQEISQLHDNAQQNQSHFVLLERRFSRLQSFNDEPQLQDYRLQLEHDDAVVKQIAQLRQVANAALCDYEKHQVC  90
Y2836-CntL/1-265       1 MYTLMKADVLAQLAGLQQEISQLHDNAQQNQSHFVLLERRFSRLQSFNDEPQLQDYRLQLEHDDAVVKQIAQLRQVANAALCDYEKHQVC  90

YPTB1372-CntL/1-265   91 ALCGPSSKTDDYLTSFNQSLQQEIKLAGMQMGEKVLLVGSGALPTTALVLVAKLGATVFCYDHDPAAQQLARQLVQSLGLEKQVQFIDNL 180
Y2836-CntL/1-265      91 ALCSPSSKTDDYLTSFNQSLQQEIKLAGMQMGEKVLLVGSGALPTTALVLVAKLGATVFCYDHDPAAQQLARQLVQSLGLEKQVQFIDNL 180

YPTB1372-CntL/1-265  181 KELTDRPVDHIIVASLVADKQALLAQLVPYVTRSSKLVMRYGNGLKSIFNCPYCHEANCSHWRTASKPVTTGLYDLIILEPNHHA       265
Y2836-CntL/1-265     181 KELTDRPVDHIIVASLVADKQALLAQLVPYVTRSSKLVMRYGNGLKSIFNCPYCHEVNCSHWRTASKPVTTGLYDLIILEPNHHA       265
```

CntM

```
YPTB1373-CntM/1-456    1 ----------MHNTLPTLILGAGPAAIQLAVDISATGDARLGLYNRPSTKGERLKQYLALTPTLYLQGTGKAQATQKESSVTIDCYIDQL  80
Y2835-CntM/1-466       1 MTLSFWNLIIMHNTLPTLILGAGPAAIQLAVDISATGDARLGLYNRPSTKGERLKQYLALTPTLYLQGTGKAQATQKESSVTIDCYIDQL  90

YPTB1373-CntM/1-456   81 AQAVGDWQRLILAVPADHYYAVLQQIPWAALPQLKSVILLSSSMGSGLMVQNLLNAAGKRDVEVISLSSYYADTKYIRAETQDISANTQD 170
Y2835-CntM/1-466      91 AQAVGDWQRLILAVPADHYYAVLQQIPWAALPQLKSVILLSSSMGSGLMVQNLLNAAGKRDVEVISLSSYYADTKYIRAETQDISANTQD 180

YPTB1373-CntM/1-456  171 INAGTQDIGAIQPYRAYTKAFKQRIYLANQWGNAGSAEMSWLTAVLARHHIDTLPCSNLLAAERFSITNYVHPPLALADTTLQALFYPEQ 260
Y2835-CntM/1-466     181 INAGTQDIGAIQPYRAYTKAFKQRIYLANQWGNAGSAEMSWLTAVLARHHIDTLPCSNLLAAERFSITNYVHPPLALADTTLQALFYPEQ 270

YPTB1373-CntM/1-456  261 RSQYLYKTQPEGPVCPAVIADLAGLADDYKRLLNRLGVEEINLLRFLNDDNYPVPASMVSRRWIDEFPQLPPLEQQYALFVRYTALLVDP 350
Y2835-CntM/1-466     271 RSQYLYKTQPEGPVCPAVIADLAGLADDYKRLLNRLGVEEINLLRFLNDDNYPVPASMVSRRWIDEFPQLPPLEQQYALFVRYTALLVDP 360

YPTB1373-CntM/1-456  351 YSTPDEQGRFYDFSAVKVATVYQDANALWHLPRVPLEDVHKLRTLLLLAGALDVVMPTAQRLLQRFQQALKAFIDRVGEEHCHPSLLGDD 440
Y2835-CntM/1-466     361 YSTPDEQGRFYDFSAVKVATVYQDANALWHLPRVPLEDVHKLRTLLLLAGALDVVMPTAQRLLQRFQQALKAFIDRVGEEHCHPSLLGDD 450

YPTB1373-CntM/1-456  441 CDRQAAIIEQQWRSQT                                                                            456
Y2835-CntM/1-466     451 CDRQAAIIEQQWRSQT                                                                            466
```

CntI

```
YPTB1374-CntI/1-281    1 -----MNQGALLAILASLIFSVMNVLVKTIADEIPTGEIVFFRSSIGCLLIGLLMYQRGIAFSREDRPLLVLRGTMGALYLICYFYSIAH  85
Y2834-CntI/1-286       1 MAEPDMNQGALLAILASLIFSVMNVLVKTIADEIPTGEIVFFRSSIGCLLIGLLMYQRGIAFSREDRPLLVLRGTMGALYLICYFYSIAH  90

YPTB1374-CntI/1-281   86 LTLADASMLAYLSPFFSIVLSLLVLRERVNATMAFWLVMVIIGAIILIRPWNFSTYTLASLVGVMSAVFAAIAYLSVNKLTKRHHNYEIV 175
Y2834-CntI/1-286      91 LTLADASMLAYLSPFFSIVLSLLVLRERVNATMAFWLVMVIIGAIILIRPWNFSTYTLASLVGVMSAVFAAIAYLSVNKLTKRHHNYEIV 180

YPTB1374-CntI/1-281  176 FYFLFIATLISIPLMWHNFVWPSGYQFGILIAIALVSLLGQVVLTQAFSSDNLIVVSVVRYIGIVFNITWGWLFWDEVPLMLSLMGGGLV 265
Y2834-CntI/1-286     181 FYFLFIATLISIPLMWHNFVWPSGYQFGILIAIALVSLLGQVVLTQAFSSDNLIVVSVVRYIGIVFNITWGWLFWDEVPLMLSLMGGGLV 270

YPTB1374-CntI/1-281  266 VVSCIQLGLRSKKKAA                                                                            281
Y2834-CntI/1-286     271 VVSCIQLGLRSKKKAA                                                                            286
```

Supplementary Figure 1. Sequence conservation between the different predicted cnt genes in *Y. pestis* and *Y. pseudotuberculosis*.

	YPTB1370	YP2838-40
ipTM	-	0.48 (Very low)
pTM	0.93 (Very high)	0.48 (Very low)

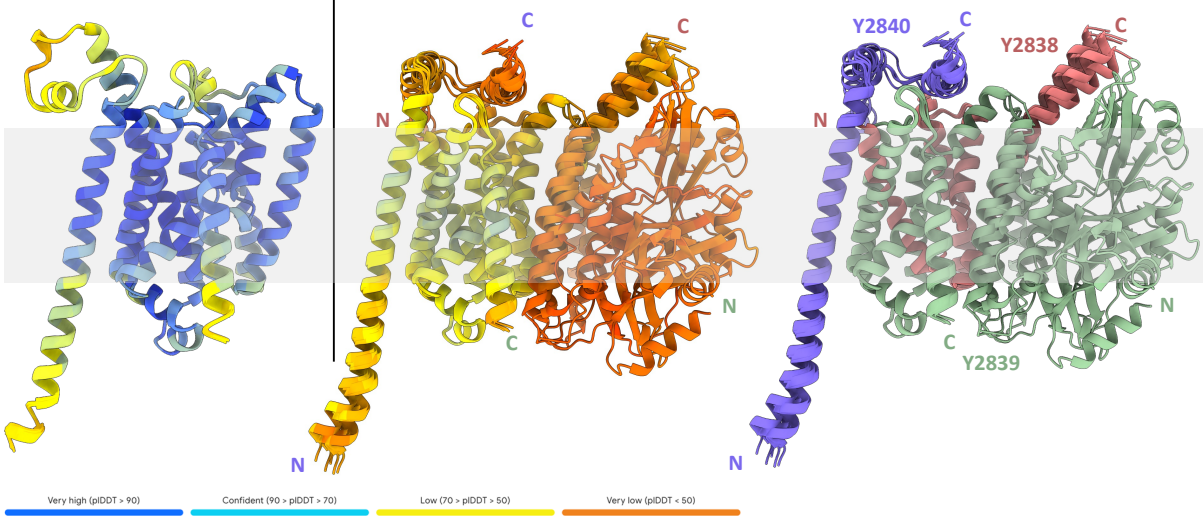

Supplementary Figure 2. AlphaFold3 models of a CntQ monomer from *Y. pseudotuberculosis* (YPTB1370; left) and *Y. pestis* (YP2838-40; right). The models are coloured according to the quality of the prediction, except for the right panel, which shows the position of the three peptides and the location of their N- and C-terminus. The approximate position of the membrane is shown in grey.

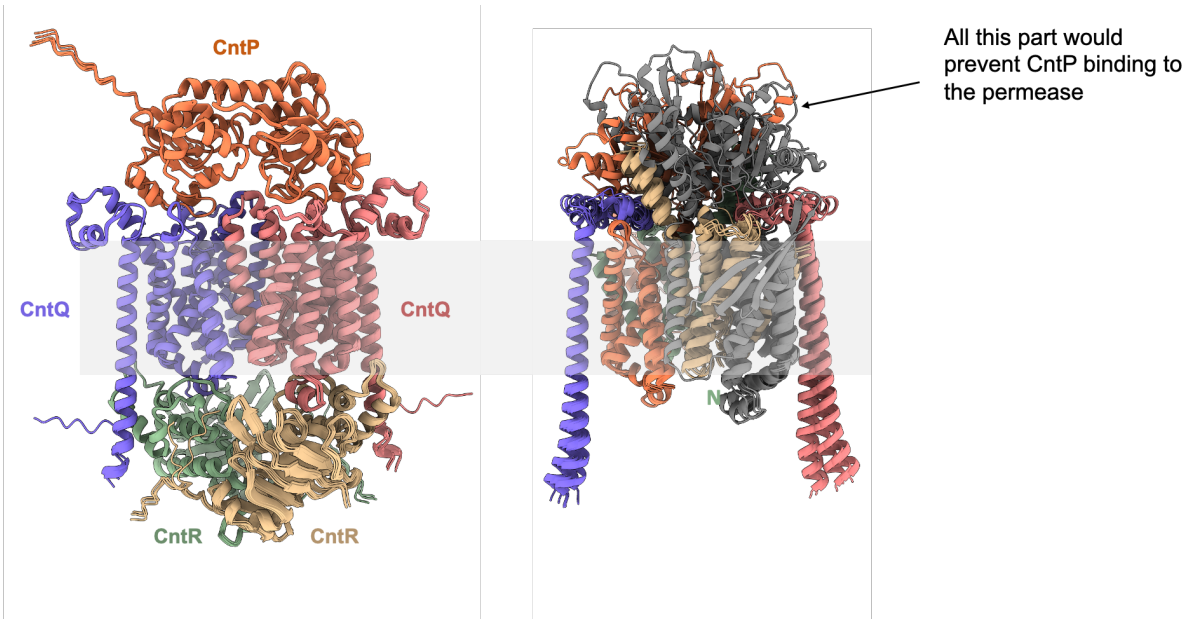

Supplementary Figure 3. AlphaFold3 models of the CntPQ$_2$R$_2$ from *Y. pseudotuberculosis* (left ; ipTM = 0.81 pTM = 0.84) and the CntQ$_2$ from *Y. pestis* (right ; ipTM = 0.61 pTM = 0.61). Although there would be enough space for interaction with the ATPase CntR in the cytoplasm, the space used for recognition of CntP in the periplasm is occupied by additional peptide parts that have no counterpart in *Y. pseudotuberculosis*, therefore leading to our central hypothesis that the three peptides produced by Y. pestis (Y2838-40), even if produced, are likely non-functional.

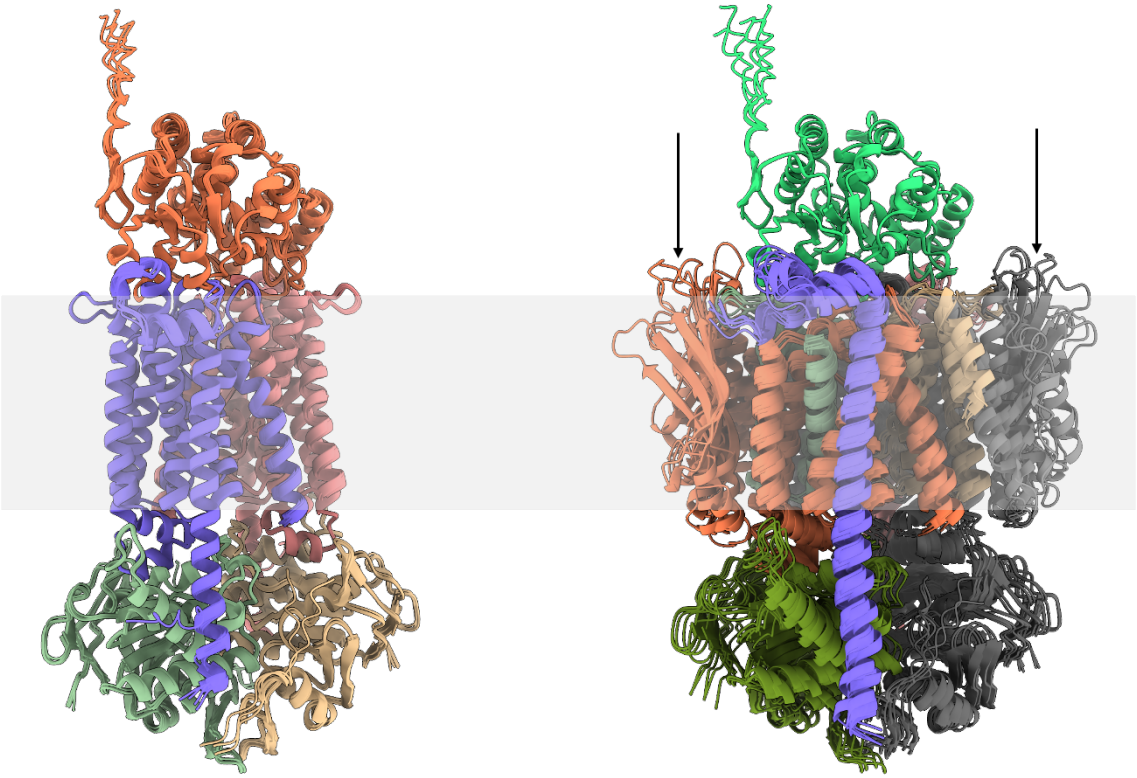

Supplementary Figure 4. AlphaFold3 models of the $CntPQ_2R_2$ from *Y. pseudotuberculosis* (left; ipTM = 0.81 pTM = 0.84) and the equivalent from *Y. pestis* (right; ipTM = 0.65 pTM = 0.65). With regard to *Y. pestis*, the modelling with CntP indicates that the parts that have no equivalent in *Y. pseudotuberculosis* now folds in the membrane (arrows), most probably because the model forces CntP binding. However, if stable, this part should fold in the periplamic space, which should therefore prevent either membrane insertion of CntQ or CntP binding to CntQ, anyway likely impairing its function.

522

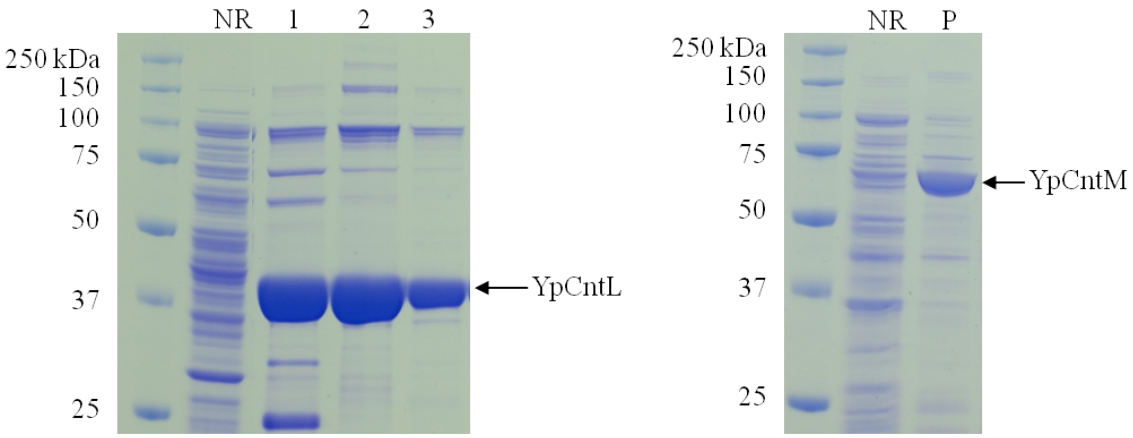

523 **Supplementary Figure 5**: SDS-PAGE gels illustrating the purifications of YpCntL (left) and YpCntM
524 (right) using HisTrap columns. NR corresponds to the flow-through fraction, 1, 2 and 3 to the different
525 eluted fractions, and P to the eluted fraction of CntM.

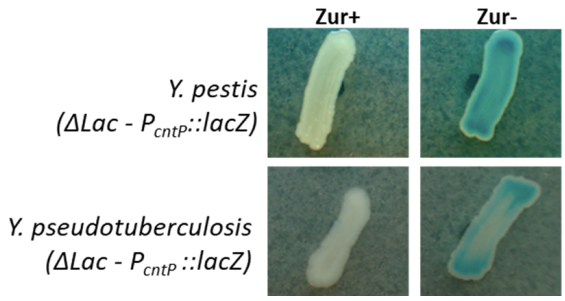

Supplementary Figure 6. Zur-dependent repression of the *cnt* operon in *Y. pestis* and *Y. pseudotuberculosis*. *Y. pestis* and *Y. pseudotuberculosis* Δ*lacZ* strains, either expressing (+) or lacking (-) Zur, carried a chromosomal fusion between the *cnt* operon promoter (P_{cntP}) and the *E. coli lacZ* reporter gene. Promoter activity was assessed by β-galactosidase activity, visualized as blue coloration on LB agar plates supplemented with X-gal.

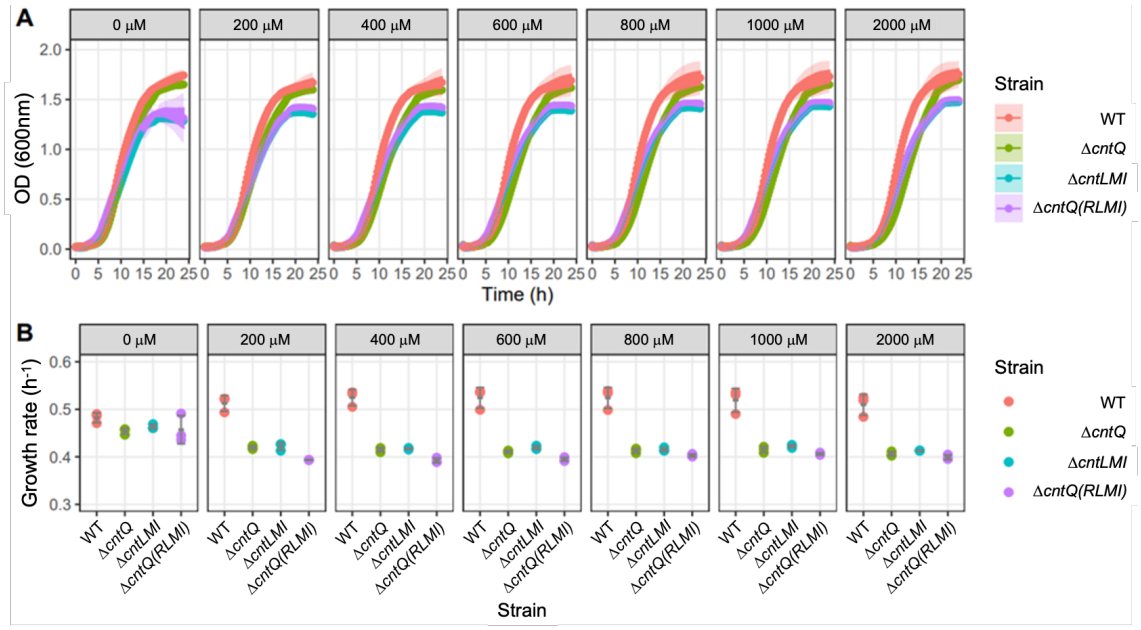

Supplementary Figure 7: Growth curves (A) and inferred growth rates (B) of *Y. pseudotuberculosis* cultivated in TMH without or with increasing concentration of EDTA. In A, the data represent the means and the confidence intervals (95%) calculated from three biological replicates. In B, the data from these three biological replicates are shown as individual points associated with their mean and standard deviation (in grey).

Organism	Label	maxLrap	minLrap	Ident %	Eval	OrderQ	OrderB	BeginQ	EndQ	LengthQ	BeginB	EndB	LengthB
Yersinia pseudotuberculosis IP 32953	YPTB1370	1,00	1,00	100	2,42E-192	1	1	1	352	352	1	352	352
Yersinia pseudotuberculosis PB1/+	YPTS_1469	1,00	1,00	100	2,42E-192	1	1	1	352	352	1	352	352
Yersinia pseudotuberculosis YPIII	YPK_2719	1,00	1,00	99	9,13E-192	1	1	1	352	352	1	352	352
Yersinia pseudotuberculosis IP 31758	YpsIP31758_2634	1,00	1,00	99	3,50E-191	1	1	1	352	352	1	352	352
Yersinia pestis Nepal516	YPN_2640	0,46	0,54	100	1,46E-85	1	1	190	352	352	138	300	300
Yersinia pestis Nepal516	YERNE_2722	0,31	0,86	99	1,33E-54	3	1	79	188	352	1	110	128
Yersinia pestis Nepal516	YERNE_2723	0,20	0,92	97	1,30E-33	8	1	1	72	352	1	72	78
Yersinia pestis CO92	YPO1344	0,46	0,54	100	1,50E-85	1	1	190	352	352	139	301	301
Yersinia pestis CO92	YERPE_1369	0,31	0,86	99	1,37E-54	3	1	79	188	352	1	110	128
Yersinia pestis CO92	YERPE_1368	0,20	0,92	97	1,33E-33	8	1	1	72	352	1	72	78
Yersinia pestis KIM	y2839	0,46	0,58	100	1,49E-85	1	1	190	352	352	118	280	280
Yersinia pestis KIM	y2838	0,32	0,86	99	7,22E-56	3	1	77	188	352	1	112	130
Yersinia pestis KIM	y2840	0,20	0,87	97	1,32E-33	8	1	1	72	352	6	77	83
Yersinia pestis D106004	YPD4_1189	0,45	1,00	100	8,95E-83	1	1	195	352	352	1	158	158
Yersinia pestis D106004	YPD4_1188	0,31	0,86	99	1,35E-54	3	1	79	188	352	1	110	128
Yersinia pestis D106004	YERPDc_1422	0,20	0,92	97	1,31E-33	8	1	1	72	352	1	72	78
Yersinia pestis biovar Orientalis PEXU2	YERP2_13281	0,45	1,00	100	9,22E-83	1	1	195	352	352	1	158	158
Yersinia pestis biovar Orientalis PEXU2	YERP2_13280	0,31	0,86	99	1,39E-54	3	1	79	188	352	1	110	128
Yersinia pestis biovar Orientalis PEXU2	YERP2_13279	0,20	0,92	97	1,35E-33	8	1	1	72	352	1	72	78
Yersinia pestis biovar Mediaevalis K1973002	YERPM_20240	0,40	1,00	100	3,81E-73	1	1	211	352	352	1	142	142
Yersinia pestis biovar Mediaevalis K1973002	YERPM_20241	0,31	0,86	99	1,36E-54	3	1	79	188	352	1	110	128
Yersinia pestis biovar Mediaevalis K1973002	YERPM_20242	0,20	0,92	97	1,32E-33	8	1	1	72	352	1	72	78
Yersinia pestis biovar Orientalis F1991016	YERPF_10236	0,40	1,00	100	3,93E-73	1	1	211	352	352	1	142	142
Yersinia pestis biovar Orientalis F1991016	YERPF_10237	0,31	0,86	99	1,40E-54	3	1	79	188	352	1	110	128
Yersinia pestis biovar Orientalis F1991016	YERPF_10238	0,20	0,92	97	1,37E-33	8	1	1	72	352	1	72	78
Yersinia pestis biovar Orientalis India 195	YERPO_90280	0,45	1,00	100	9,05E-83	1	1	195	352	352	1	158	158
Yersinia pestis biovar Orientalis India 195	YERPO_90279	0,31	0,86	99	1,36E-54	3	1	79	188	352	1	110	128
Yersinia pestis biovar Orientalis India 195	YERPO_90278	0,20	0,92	97	1,33E-33	8	1	1	72	352	1	72	78
Yersinia pestis biovar Antiqua B42003004	YERP4_20352	0,45	1,00	100	9,33E-83	1	1	195	352	352	1	158	158
Yersinia pestis biovar Antiqua B42003004	YERP4_20350	0,20	0,92	97	1,37E-33	8	1	1	72	352	1	72	78
Yersinia pestis biovar Antiqua B42003004	YERP4_20351	0,32	0,86	99	7,45E-56	3	1	77	188	352	1	112	130
Yersinia pestis CA88-4125	YERPCc_20318	0,45	1,00	100	9,02E-83	1	1	195	352	352	1	158	158
Yersinia pestis CA88-4125	YERPCc_20317	0,31	0,86	99	1,36E-54	3	1	79	188	352	1	110	128
Yersinia pestis CA88-4125	YERPCc_20316	0,20	0,92	97	1,32E-33	8	1	1	72	352	1	72	78
Yersinia pestis Pestoides F	YPDSF_2355	0,46	0,54	100	1,45E-85	1	1	190	352	352	138	300	300
Yersinia pestis Pestoides F	YERPN_2489	0,31	0,86	99	1,32E-54	3	1	79	188	352	1	110	128
Yersinia pestis Pestoides F	YERPN_2490	0,20	0,92	97	1,29E-33	8	1	1	72	352	1	72	78
Yersinia pestis D182038	YPD8_0957	0,45	1,00	100	8,87E-83	1	1	195	352	352	1	158	158
Yersinia pestis D182038	YERP1c_1143	0,31	0,86	99	1,34E-54	3	1	79	188	352	1	110	128
Yersinia pestis D182038	YERP1c_1144	0,20	0,92	97	1,30E-33	8	1	1	72	352	1	72	78
Yersinia pestis biovar Antiqua E1979001	YERP9_50170	0,45	1,00	100	9,32E-83	1	1	195	352	352	1	158	158
Yersinia pestis biovar Antiqua E1979001	YERP9_50169	0,31	0,86	99	1,40E-54	3	1	79	188	352	1	110	128
Yersinia pestis biovar Antiqua E1979001	YERP9_50168	0,20	0,92	97	1,36E-33	8	1	1	72	352	1	72	78
Yersinia pestis biovar Microtus str, 91001	YP_1252	0,46	0,58	100	1,49E-85	1	1	190	352	352	118	280	280
Yersinia pestis biovar Microtus str, 91001	YER91_1269	0,31	0,86	99	1,36E-54	3	1	79	188	352	1	110	128
Yersinia pestis biovar Microtus str, 91001	YER91_1270	0,20	0,92	97	1,33E-33	8	1	1	72	352	1	72	78
Yersinia pestis Angola	YpAngola_A1574	0,41	1,00	100	6,57E-75	1	1	208	352	352	1	145	145
Yersinia pestis Angola	YpAngola_A1574	0,32	0,86	99	6,83E-56	3	1	77	188	352	1	112	130
Yersinia pestis Angola	YpAngola_A1574	0,20	0,92	97	1,25E-33	8	1	1	72	352	1	72	78
Yersinia pestis Antiqua	YPA_0630	0,46	0,54	100	1,52E-85	1	1	190	352	352	138	300	300
Yersinia pestis Antiqua	YERPA_0653	0,31	0,86	99	1,38E-54	3	1	79	188	352	1	110	128
Yersinia pestis Antiqua	YERPA_0652	0,20	0,92	97	1,35E-33	8	1	1	72	352	1	72	78
Yersinia pestis Pestoides A	YERPPA_250040	0,30	1,00	100	8,39E-52	3	1	248	352	352	1	105	105
Yersinia pestis Pestoides A	YERPPA_250038	0,31	0,86	99	1,38E-54	2	1	79	188	352	1	110	128
Yersinia pestis Pestoides A	YERPPA_250037	0,20	0,92	97	1,35E-33	8	1	1	72	352	1	72	78
Yersinia pestis biovar Antiqua UG05-0454	YERPU_20097	0,40	1,00	100	3,88E-73	1	1	211	352	352	1	142	142
Yersinia pestis biovar Antiqua UG05-0454	YERPU_20098	0,31	0,86	99	1,39E-54	3	1	79	188	352	1	110	128
Yersinia pestis biovar Antiqua UG05-0454	YERPU_20099	0,20	0,92	97	1,35E-33	8	1	1	72	352	1	72	78

Supplementary Table 1. Pseudogenization of the *cntQ* permease is conserved in *Y. pestis* strains. List of orfs predicted in sequenced *Y. pseudotuberculosis* and *Y. pestis* strains at the *cntQ* position. maxLrap and minLrap denote respectively the length (expressed as a percentage of the gene) that is conserved, taking YPTB1370 as a reference (Query). BeginQ and EndQ refer to portions of sequence that is conserved on YPTB1370, taking YPTB1370 (Query) as a reference. BeginB and EndB refer to portions of sequence that is conserved in a given sequence (Bait), using YPTB1370 as a reference.

549 **Supplementary Table 2. Bacterial strains and plasmids used in this study**

Strain name in the text	*Description*
Yersinia pseudotuberculosis	
Y. pseudotuberculosis WT	*Y. pseudotuberculosis* IP32777
Y. pseudotuberculosis Δ*lacZ* P_{cntP}::*lacZ* (Zur+)	IP32777 Δ*lacZ* P_{cntP}::*lacZ* chromosomal *lacZ* reporter fusion with *cnt* promoter
Y. pseudotuberculosis Δ*lacZ* P_{cntP}::*lacZ* (Zur-)	IP32777 Δ*lacZ* Δ*zur* P_{cntP}::*lacZ* *zur* deletion and *lacZ* reporter fusion with *cnt* promoter
Y. pseudotuberculosis ΔcntLMI	IP32777 Δ*cntLMI*-FRT unlabeled deletion of *cntLMI*
Y. pseudotuberculosis ΔcntQ(RLMI)	IP32777 Δ*cntQ*::Km1447 *cntQ* deletion and insertion of a kanamycin resistance cassette abolishing *cntRLMI* expression
Y. pseudotuberculosis ΔcntQ	IP32777 Δ*cntQ*-FRT unlabeled deletion of *cntQ,* no polar effect on *cntRLMI* downstream genes
Y. pseudotuberculosis ΔcntQ(RLMI) complemented	IP32777 Δ*cntQ*::Km1447 mini-Tn7-Zeo2::*cntPQRLMI* Strain complemented by the insertion of *cntPQRLMI*
Yersinia pestis	
Y. pestis WT	*Y. pestis* KIM6+
Y. pestis ΔcntLMI	KIM6+ Δ*cntLMI*::Tp1087 *cntLMI* deletion and insertion of a trimethoprim (Tp) resistance cassette
Y. pestis ΔcntQ(RLMI)	KIM6+ Δ*cntQ*::Km1447 *cntQ* deletion and insertion of a kanamycin resistance cassette abolishing *cntRLMI* expression
Y. pestis Δ*lacZ* P_{cntP}::*lacZ* (Zur+)	KIM6+ Δ*lacZ* P_{cntP}::*lacZ* chromosomal *lacZ* reporter fusion with *cnt* promoter
Y. pestis Δ*lacZ* P_{cntP}::*lacZ* (Zur-)	KIM6+ Δ*lacZ* Δ*zur* P_{cntP}::*lacZ* *zur* deletion and *lacZ* reporter fusion with *cnt* promoter
Y. pestis ΔcntQ(RLMI) ΔybtX	KIM6+ Δ*cntQ*::Km1447 Δ*ybtX*::TpNP *ybtX* deletion and insertion of a Tp resistance cassette without polar effect on downstream *ybt* genes
Y. pestis ΔcntLMI ΔznuCB	KIM6+ Δ*cntLMI*::Tp1087 Δ*znuCB*::Km4 Deletion of *znuCB* and insertion of a kanamycin resistance cassette
Y. pestis ΔcntQ(RLMI) ΔybtX ΔznuCB	KIM6+ Δ*cntQ*::Km1447 Δ*ybtX*::TpNP Δ*znuCB*::Sm1315 Deletion of *znuCB* and inserting a streptomycin resistance cassette

Plasmids

Name	Description	Reference
pACYC177	Suicide plasmid used as a template to generate pEP699 by ExoCET cloning.	(Rose 1988)
pDS132	Suicide plasmid, CmR.	(Philippe et al. 2004)
pFLP3	Encodes FLP recombinase to excise FRT flanked cassettes.	(Choi et al. 2005)
pKD4	Source of KmR cassette, Km flanked by FRT sites.	(Datsenko and Wanner 2000)
pEP620	lacZ reporter suicide plasmid bearing P_{cnt} from *Y. pestis*, KmR	This work
pEP681	pDS132:: DcntQ::Km1447, CmR KmR	This work
pEP692	pDS132::DcntLMI::Tp1087, CmR TpR	This work
pEP696	lacZ reporter suicide plasmid bearing Pcnt from *Y. pseudotuberculosis*, derived from pEP848, KmR	This work
pEP699	p15A-Ap::cntPQRLMI, obtained by ExoCET cloning of the *Y. pseudotuberculosis cnt* operon, AmpR	This work
pEP701	pUC18R6K-miniTn7-Zeo2-cntPQRLMI, bears the *Y. pseudotuberculosis cnt* operon, AmpR ZeoR	This work
pEP848	lacZ reporter suicide plasmid, KmR	EP collection
pEP1046	pUC18R6K-miniTn7-Zeo2, used to clone the *Y. pseudotuberculosis cnt* operon, AmpR ZeoR	GenBank MH614591
pEP1087	Source of TpR cassette flanked by FRT sites	(Bibi-Triki et al. 2014)
pEP1315	Source of SmR cassette flanked by FRT sites	GenBank MH626523
pEP1436	Plasmid used for Red recombination in *Y. pestis*	(Dewitte et al. 2020)
pEP1447	Source of Km1447 cassette flanked by FRT sites, in this plasmid the Km resistance gene is oriented opposite to that in pEP1446	EP collection

550

551

552 **Supplementary Table 3. Composition of the TMH medium**

Compound	Final concentration (mM)
DL-Ala	2.5
L-Ile	1
L-Val	1
L-Leu	1
L-Phe	1
L-Tyr	1
L-Thr	5
L-Arg	1
L-Pro	5
L-Glu	5
L-Lys	1
Gly	5
L-His	1
L-Asp	2
L-Ser	5
L-Trp	0.1
L-Asn	2.5
L-Gln	10
L-Met	1
Sodium thiosulfate	2.5
KH_2PO_4	2.5
Citric acid	10
NH_4Cl	10
$MnCl_2$	0.01
$FeCl_2$	0.1
$MgCl_2$	20
HEPES	25
Thiamine (vit. b2)	0.0003
Panthotenic acid (vit. b5)	0.0004
Biotine (vit. b8)	0.0002
Potassium gluconate	10

553
554

555 **Supplementary Table 4. Metal concentrations in TMH medium.** Metal
556 concentration as determined by ICP-AES (Bdl: below detection level).

Metal	Concentration (μM)
Mn	6.3
Fe	62.5
Zn	Bdl
Cu	Bdl
Ni	Bdl
Co	Bdl

557

558 **Supplementary References**

559 Bibi-Triki S, Li de la Sierra-Gallay I, Lazar N, et al (2014) Functional and Structural
560 Analysis of HicA3-HicB3, a Novel Toxin-Antitoxin System of *Yersinia pestis*.
561 Journal of Bacteriology 196:3712–3723. https://doi.org/10.1128/JB.01932-14

562 Choi K-H, Gaynor JB, White KG, et al (2005) A Tn7-based broad-range bacterial
563 cloning and expression system. Nat Methods 2:443–448.
564 https://doi.org/10.1038/nmeth765

565 Datsenko KA, Wanner BL (2000) One-step inactivation of chromosomal genes in
566 *Escherichia coli* K-12 using PCR products. Proceedings of the National Academy
567 of Sciences 97:6640–6645. https://doi.org/10.1073/pnas.120163297

568 Dewitte A, Bouvenot T, Pierre F, et al (2020) A refined model of how *Yersinia pestis*
569 produces a transmissible infection in its flea vector. PLOS Pathogens 16:e1008440.
570 https://doi.org/10.1371/journal.ppat.1008440

571 Philippe N, Alcaraz J-P, Coursange E, et al (2004) Improvement of pCVD442, a suicide
572 plasmid for gene allele exchange in bacteria. Plasmid 51:246–255.
573 https://doi.org/10.1016/j.plasmid.2004.02.003

574 Rose RE (1988) The nucleotide sequence of pACYC177. Nucleic Acids Research
575 16:356. https://doi.org/10.1093/nar/16.1.356

576

577